

# Fluid flow and static structural analysis of E-glass versus S-glass fibre/epoxy reinforced composite pipe joints

Sujith Bobba<sup>1\*</sup>, Z. Leman<sup>1,2</sup>, E. S. Zainudin<sup>1</sup>, S. M. Sapuan<sup>1,2</sup>

(1. *Department of Mechanical and Manufacturing Engineering, Faculty of Engineering, Universiti Putra Malaysia, 43400 Serdang, Malaysia;*

2. *Laboratory of Biocomposite Technology, Institute of Tropical Forestry and Forest Products (INTROP), Universiti Putra Malaysia, 43400 Serdang, Malaysia)*

**Abstract:** Glass fiber/epoxy reinforced composite pipes are commonly used in the industry where circulation of extreme forced chemical fluids, industrial wastes and oil and natural gas transmission occurs. In oil and natural gas production, the heavy crude oil transporting pipe lines are exposed to unsteady pressure waves which generate rise and fall stress readings in the pipes. Computational fluid dynamic examination was implemented using Ansys 15.0 Fluent software to investigate the consequences of these pressure waves on some detailed joints in the pipes. Relating on the type of heavy crude oil being employed, the flow behaviour stated a significant degree of stress levels in evident attaching joints, triggering the joints to become delicate over a sustained phase of usage. In this analysis, the comparison among various pipe joints was done by using different materials, and the end result of the stress volume in the pipe joints was checked so that the life of the pipe joints can be optimized by the change of material.

**Keywords:** glass/epoxy fibre reinforced composite pipes, heavy crude oil, pressure waves, computational fluid dynamics

**Citation:** Bobba, S., Z. Leman, E. S. Zainudin, and S. M. Sapuan. 2019. Fluid flow and static structural analysis of E-glass versus S-glass fibre/epoxy reinforced composite pipe joints. *Agricultural Engineering International: CIGR Journal*, 21(4): 56–63.

## 1 Introduction

The most commonly used pipe systems for fluid transportation are constructed by glass fiber reinforced plastic composites, also known as fiber glass composites. In other terms, infrastructural industries can be regarded as the those who introduced a method for using composite materials in eradicating corrosion in chemically sensitive environments, and its consequential service costs are the major causes that various industrial divisions have been encouraged to implement glass/epoxy fibre reinforced pipes (Hollaway, 2010). Glass/epoxy fiber reinforced pipes and pipe joints are imposed to stay in action for 65 years as an extended stage design limitation controlled by international rules and

regulations (AWWA Manual M45, 2005; ANSI/AWWA C950-0,1 2001). More or less all the conducted studies in the literature on the distinguish design behaviour of glass/epoxy fibre reinforced pipes exposed to internal pressure have been diffused out experimentally (Abdul Majid et al., 2014; Gay et al., 2002) but not on pipe joints where the flow is turbulent.

Subsea pipeline system is used to connect the offshore production platforms to onshore production platforms. Inspection of the pipe line system is done on regular basis, but danger is not predicted and the failure of the system may occur in few cases.

### 1.1 Analysis of significant pipe joint failures

Pipe failures are generated by concern forces which over reach the normal residual strength of the pipe medium. Pipe deterioration happens when the stresses of both operative and environmental react on pipe lines where corrosion, deterioration, insufficient installation or manufacturing problems have influenced the pipes structural strength. The physical process of failures in

**Received date:** 2018-10-29 **Accepted date:** 2019-01-03

**\*Corresponding author:** Sujith Bobba, Research scholar, Department of Mechanical and Manufacturing Engineering, Faculty of Engineering, Universiti Putra Malaysia, 43400 Serdang, Malaysia. Tel: +60104339673, Email: [sujith.bobba@mail.com](mailto:sujith.bobba@mail.com).

pipe lines is normally a complicated function of many subscribing factors. This shows pipe line properties such as area, material, internal and external storing and environmental issue (Xia et al., 2001). Consequently, various other failure localities can be noticed including joint contact failure, breakable failure, crack pipe, transversal break, graphitization, pitting holes, long term and circumferential failures, circular cracking and finally blowout hole. When comparing the aspects for failure, physical characteristics such as material type, size and temperature have been analysed as the most prominent factors.

In the case of structural stress analysis, Xia M et al. (2001), Akkus and Kawahara (2000) have found out two approaches to figure out stresses and variations of filament wound pipe joints which were exposed to cross loading employing arched composite beam and bi-layer build up approaches. Various studies were conducted on glass fiber reinforced plastic pipe's mechanical, structural properties and break down such as bending (Alderson and Evans, 1992), transverse loading (Nishiwaki et al., 1995; Onoda, 1985) and axial compression (Smerdov, 2000) loading circumstances regularly. Moujaes and Aekula (2009) stated that the consequences of the drop in pressure on the turning vanes were 90 degree, by means of computational fluid dynamics stimulations in heating, ventilation and air conditioning applications field. Stress examination of even pipe bends with end restraints exposed and flanged to in level bending investigated experimentally by Hilsenkopf et al. (1998), Kim and Oh (2007) has provided a method to calculate approximately plastic capacities for elbows with non-uniform thickness under in-plane bending and below internal pressure, built on the finite element boundary analysis by means of elastic-plastic materials

## 1.2 Influence of pressure variation on pipe joint failure

The expression for pressure variation is used to point out any development in pressure level in the pipelines, either a slow advancement in the day to day pressure analysis or sudden change in pressure short term events. These bear to have a duplicating sequence, even though there might be much change in the magnitude, frequency

and structure of every incident. In supplement, separation of pressure variation levels from other level on an instant phase can be highly challenging. However, there have been only few past studies on the failure mechanism of pipelines when they are defined to the constant cycles of pressure variations. In the study, common pipeline side by side of the crude oil delivery structure will be unprotected to different pressure constantly. Same to immediate pressure variation, the relationship between (continuous) pressure change and the main cause of failure is not perfectly understood.

The flow range sometimes can be impeded due to the displacement of consecutive layers (fiber/resin) of the component and the burst pressure of the pipe joint increases due to block and the failure might occur. The influence of impact failure due to burst pressure can be evaluated by decreasing the burst pressure and increasing impact energy as per the studies done by various researchers (Mazumder, 2012).

## 2 CFD modelling of the pipe joints

### 2.1 Design of the pipe joints

It should be pointed out that all designed glass-reinforced plastic, glass reinforced vent and glass reinforced epoxy pipes with filament winding method have the similar pipe wall layout and thickness. However, for the case of glass reinforced vent and glass reinforced epoxy pipes, most commonly in pure glass fiber reinforced pipe layers are used, and sand cover was placed into glass fiber reinforced pipes for the water or excess water movement applications and also in some cases depletion of the wall width is common in the initial stage of unpredicted events, since it causes local stress absorption. For the analysis part of the pipe joints such as T-joint, elbow joint, four way joints design are done as per ASME B31.3 Process Piping Code with 94.6 mm inner diameter, 100 mm outer diameter, thickness of the pipe of 5.4 mm, radius of curvature of 75 mm and 100 mm longitudinal length on each side of the joint was as shown in Figure 1. The material used is one with E-glass fiber and another with S-glass fibre. The material's properties of S-Glass and E-glass used for the design are shown in Table 1.

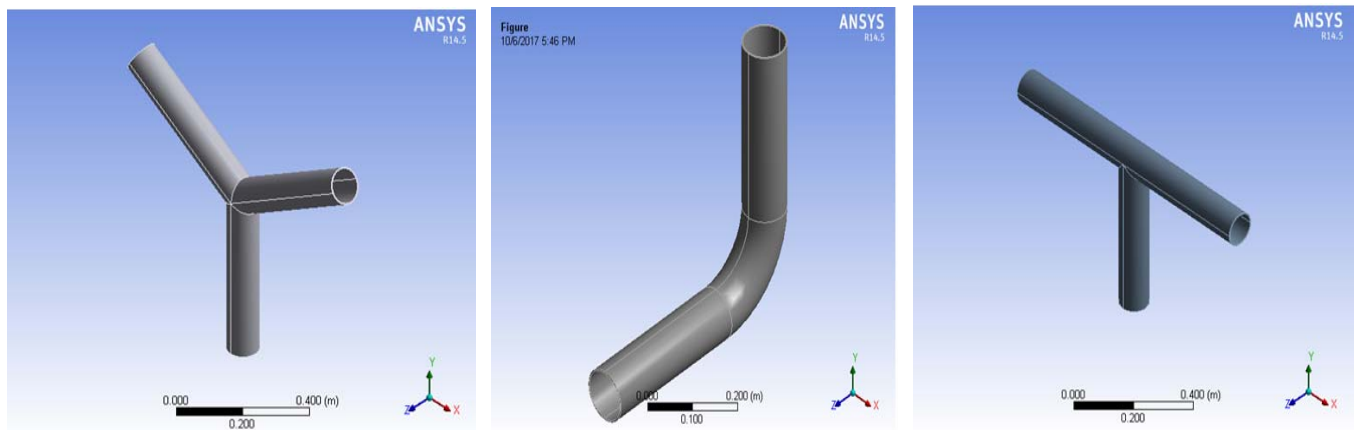


Figure 1 Design of pipe joints with required dimensions in Ansys 15.0 Work bench

**Table 1** Material properties of S-Glass and E-glass used for design

S.No	Property	S-Glass	E-Glass
1	Density	2.49 g cm <sup>-3</sup>	2.55 g cm <sup>-3</sup>
2	Possion's ratio	0.22	0.22
3	Shear Modulus	37 GPa	34 GPa
4	Young's Modulus	89 GPa	79 GPa
5	Compression strength	4500 MPa	4500 MPa
6	Tensile strength	4750 MPa	2000 MPa

## 2.2 Turbulence flow modeling in the pipe joints

The complications initiating from the surroundings of the turbulent flows are confrontationally not stable by type and the main levels that are needed to be determined are both significant and extremely minor turbulences. Therefore, computational study is confined to use remarkably small position and time discretization, which exceeds today's computational effect.

Navier-Stokes equations (Anderson, 2009) is the only way to describe the turbulent flow in pipe joints in full aspect. The succeeding equations designate how the pressure, velocity, density and temperature of an ongoing fluid are associated.

### Continuity equation:

$$\partial \rho / \partial t + \partial(\rho u) / \partial x + \partial(\rho v) / \partial y + \partial(\rho w) / \partial z = 0 \quad (1)$$

### X - Momentum:

$$\begin{aligned} \partial(\rho u) / \partial t + \partial(\rho u^2) / \partial x + \partial(\rho uv) / \partial y + \partial(\rho uw) / \partial z \\ = -\partial p / \partial x + 1 / Re_f \{ \partial \tau_{xx} / \partial x + \partial \tau_{xy} / \partial y + \partial \tau_{xz} / \partial z \} \end{aligned} \quad (2)$$

### Y - Momentum:

$$\begin{aligned} \partial(\rho v) / \partial t + \partial(\rho uv) / \partial x + \partial(\rho v^2) / \partial y + \partial(\rho vw) / \partial z \\ = -\partial p / \partial y + 1 / Re_f \{ \partial \tau_{xy} / \partial x + \partial \tau_{yy} / \partial y + \partial \tau_{yz} / \partial z \} \end{aligned} \quad (3)$$

### Z - Momentum:

$$\begin{aligned} \partial(\rho w) / \partial t + \partial(\rho uw) / \partial x + \partial(\rho vw) / \partial y + \partial(\rho w^2) / \partial z \\ = -\partial p / \partial z + 1 / Re_f \{ \partial \tau_{xz} / \partial x + \partial \tau_{yz} / \partial y + \partial \tau_{zz} / \partial z \} \end{aligned} \quad (4)$$

### Energy:

$$\begin{aligned} \partial(Et) / \partial t + \partial(uEt) / \partial x + \partial(vEt) / \partial y + \partial(wEt) / \partial z \\ = -\partial(up) / \partial x - \partial(vp) / \partial y - \partial(wp) / \partial z - 1 / (RefPrf) \\ [\partial qx / \partial x + \partial qy / \partial y + \partial qz / \partial z] + 1 / Ref [\partial / \partial x (u\tau_{xx} + \\ v\tau_{xy} + w\tau_{xz}) + \partial / \partial y (u\tau_{xy} + v\tau_{yy} + w\tau_{yz}) + \partial / \partial z (u\tau_{xz} + \\ v\tau_{yz} + w\tau_{zz})] \end{aligned} \quad (5)$$

where,  $x, y, z$  are the co-ordinates;  $u, v, w$  are the velocity elements;  $t$  is the time in sec;  $p$  is the pressure in MPa, heat flux is denoted by  $q$  in  $W/m^2$ , density as  $\rho$  in  $kg/m^3$ ,  $Re$  represents the Reynolds number which has a resemblance constraint with the proportion of the mounting of the inertia to the flow with the viscous forces in the flow. The  $q$  parameters are the heat flux elements and  $Pr$  represents the Prandtl number which is a parallel parameter in which represents the ratio of the viscous stresses to the thermal stresses. The  $\tau$  variables are modules of the stress tensor.

The above Equations (1)-(5) are expansions of the Euler Equations and comprise the outcomes of viscosity on the flow level, and describe N-S equations with very tolerable computational grids and very minor time phases to get the entire details of a turbulent flow as shown indirect numerical simulation (DNS). Figure 2 replicates the flow chart of analysis performed in the study in both theoretical and design ways.

Figure 2 replicates the flow chart of analysis performed in the study in both theoretical and design ways.

## 3 Results and discussion

### 3.1 Flow analysis of the pipe joints

Various models (Kleiner and Rajani, 2001; Shalaby et al., 2008) based on this method including physically

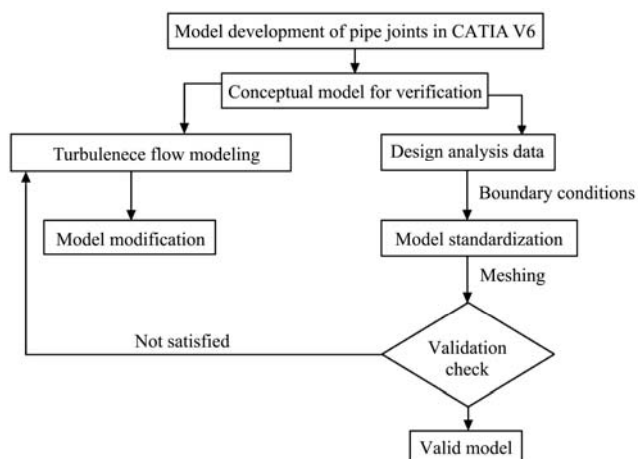


Figure 2 Basic model of simulation/flow chart for flow analysis in pipe joints with theoretical and design phases

established procedures need important data and frequently immoderate examinations on the pipe joint’s failure procedures, so flow analysis would be a source for an imaginary view of the failures before installation of the pipe joints in the pipeline system. Since the pressure flow is maximum at the joints, comparison of flow analysis between E-glass material and S-glass material has been done. The properties heavy crude oil are considered for analysis, since the fluid flowing in oil and gas industry is crude oil. The flow parameters and the thermo dynamic parameters for flow analysis are shown in Table 2 and Table 3 below. The consequence of inner pressure on failure capacity at the pipe bends under mutual moments and pressure loadings counting

geometric non linearity, have been reviewed by Shalaby and Younan et al. (2008).

**Table 2 Heavy crude oil parameters for flow analysis (Bobba et al., 2018)**

Property	Value in units
Molecular mass	0.53 kg/mol
Specific heat	1971 J kg <sup>-1</sup> at 273.3 K
Thermal conductivity	0.521 W m <sup>-1</sup> at 273.3 K
Dynamic viscosity	0.0011243 Pa s <sup>-1</sup> at 273.3 K
Specific heat ratio	1.2

**Table 3 Thermodynamic factors for flow analysis (Bobba et al., 2018)**

Parameter	Value in Units
Pressure	19432.5 Pa
Temperature	273.5 K
Mass	970 kg m <sup>-3</sup>

**Table 4 Number of elements and nodes for each joint after meshing done on the per fined pipe joints**

S.No	Type of joint	Domain	Nodes	Elements
1	Elbow-Joint	Solid	3135	2484
2	T-Joint	Solid	4792	21278
3	Y-Joint	Solid	4730	21376

### 3.1.1 Flow pressure comparison in E-glass elbow joint and S-glass elbow joint

Elbow joint with E-glass and S-glass haveequal maximum pressure of 110.3 Pa from the CFD analysis and the minimum pressure of -727.7 Pa from the CFD analysis was as shown in Figure 3.

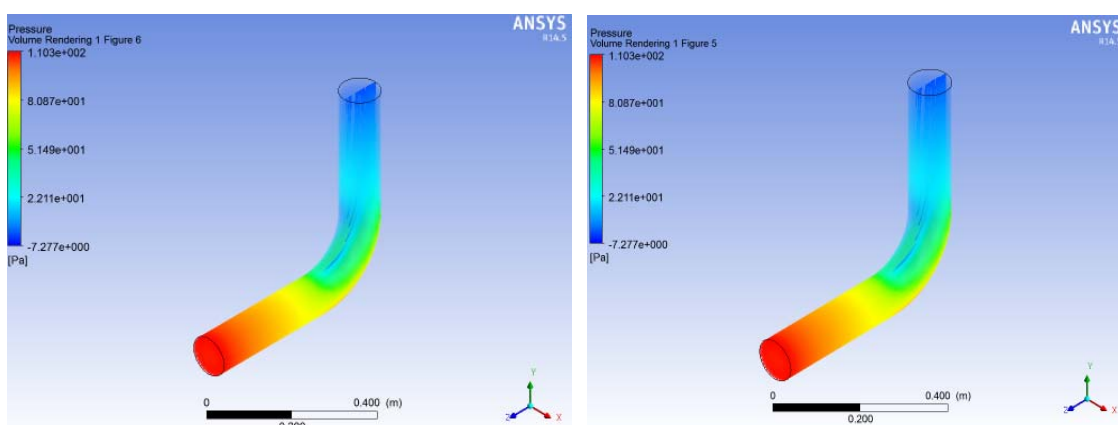


Figure 3 Comparison of pressure fluacuation between E-glass elbow joint and S-glass elbow joint through CFD analysis

### 3.1.2 Flow pressure comparison in E-glass Y-joint and S-glass Y-Joint

Y-joint made with E-glass and S-glass have equal maximum pressure of 122.1 Pa from the CFD analysis and the minimum pressure of -118.4 Pa from the CFD analysis was shown in Figure 4.

### 3.1.3 Flow pressure comparison in E-glass T-joint and S-glass T-Joint

T- Joint with E-glass and S-glass have equal maximum pressure of 147.6 Pa from the CFD analysis and the minimum pressure of -108.7 Pa from the CFD analysis was shown in Figure 5.

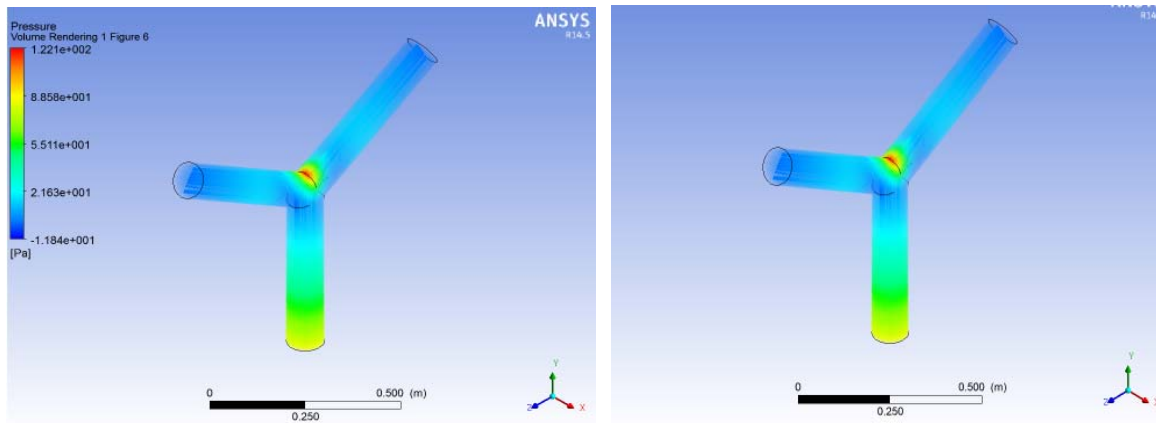


Figure 4 Comparison of pressure fluctuation between E-glass Y-joint and S-glass Y-joint through CFD analysis

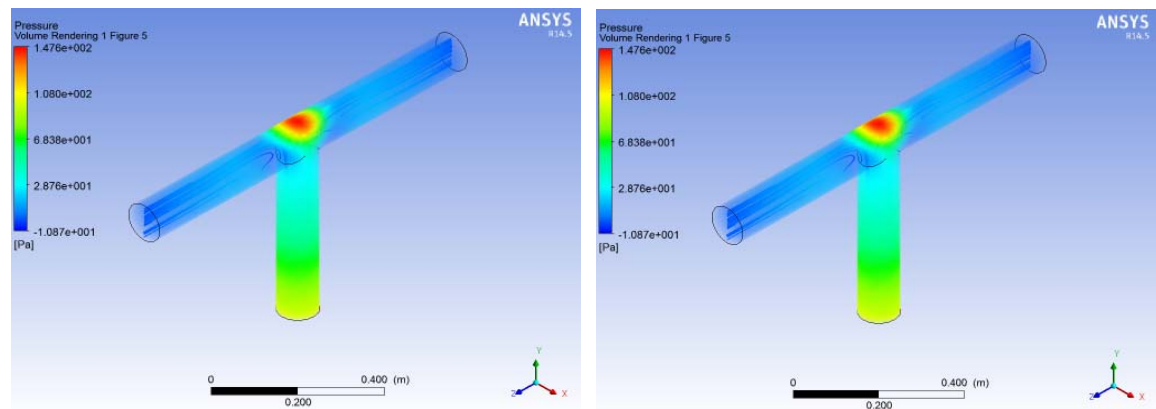


Figure 5 Comparison of pressure fluctuation between E-glass T-joint and S-glass T-joint through CFD analysis

**Table 5** Maximum and minimum pressure flow in the pipe joints

S.No	Type of Joint	Pressureflow	
		Maximum	Minimum
1	Elbow joint (S-glass/E-glass)	110.3 Pa	-727.7 Pa
2	Y-Joint (S-glass/E-glass)	122.1 Pa	-118.4 Pa
3	T-Joint (S-glass/E-glass)	147.6 Pa	-108.7 Pa

The FE patterns, shown in Figure 3, Figure 4, and Figure 5, were subjected to internal pressure. Internal pressure was employed as a circulated load to the interior cover of the FE model. In supplement, an axial tension equal to the internal pressure was employed at the tip of the pipe joint to oppose the closed end. It should be perceived that there are no complications in employing internal pressure also to the bent without any connected pipe, and the colour contours display show the pressure gets increased at the junction of three divisions of pipe joint due to which pressure loss happened in pipe joint. The velocity causes to surge at the convergence of both the pipe joints and decrease in the linking branches.

Finally, once the flow analysis was performed, the pipe joint will have much influence on the pressure surge propagation.

### 3.2 Static structural analysis of the pipe joints

#### 3.2.1 Equivalent (von mises) stress

To decrease the limitation of the pressure in the pipe joint curvature,  $P_o$ , has been classified out as:

$$P_o = \left( \sigma_o \frac{t}{r} \right) \left[ \frac{1 - \frac{r}{R}}{1 - \frac{r}{2R}} \right] \quad (6)$$

The primary phrase on the right-hand side of Equation (6) is the maximum pressure for a straight pipe joint and the second phrase is the enlargement term for the bend curvature. The first phrase is similar to a lower bound centred on the yield state of an element, and  $\frac{2}{\sqrt{3}}$  could be employed if the von mises yield situation was implemented.

$$P_o = \left( \frac{2}{\sqrt{3}} \sigma_o \frac{t}{r} \right) \left[ \frac{1 - \frac{r}{R}}{1 - \frac{r}{2R}} \right] = P_o^S \left[ \frac{1 - \frac{r}{R}}{1 - \frac{r}{2R}} \right] \quad (7)$$

where,  $P_o^S$  represents the plastic threshold pressure for the un-cracked level of the pipe joint.

Now when analysing about the extreme pressure

attained from the flow analysis of individual pipe joint shown in the Table 5, static structural and theoretical calculation to find the von mises stress was performed and compared

To calculate the equivalent von mises stress

$$\sigma_1(\text{Hoop Stress}) = \frac{P_d}{2T} \tag{8}$$

$$\sigma_2(\text{Radial Stress}) = -P \times (r_i)^2 (r_o)^2 - r^2 \times r^2 \times (r_o^2 - r_i^2) \tag{9}$$

$$\sigma_y(\text{Von Mises}) = \sqrt{\sigma_1^2 + \sigma_2^2 - 2\sigma_1\sigma_2} \tag{10}$$

where,  $P_d$  = Maximum pressure in MPa;  $r_i$  = Radius (Inner) of the pipe joint in mm;  $r_o$  = Radius (Outer) of the pipe joint in mm;  $r$  = Radius of curvature of the pipe joint in mm.

By performing theoretical calculation by exercising the above Equations (8)-(10), following results shown in Table 6 are obtained.

**Table 6 Maximum pressure flow by therotical calucations in the pipe joints**

S.No	Type of Joint	S-glass	E-glass
1	Elbow joint	87.904 Pa	88.924 Pa
2	Y-joint	85.45 Pa	97.45 Pa
3	T-joint	129.72 Pa	136.72 Pa

### 3.2.2 Finite element analysis of the pipe joints

Static analysis is performed in the case to find the given code stresses, code compliance stresses, pipe support load, element forces and moments (local and global coordinates), and the data for performing structural analysis of the pipe joints is shown in Table 7 and the number of elements and nodes for each joint are shown in Table 4.

**Table 7 Maximum equivalent (von Mises) and minimum equivalent (von Mises) stress of various joints with E-glass and S-glass fiber material**

S.No	Type of joint		S-Glass	E-Glass
1	Elbow joint	Maximum	98.904 Pa	99.924 Pa
		Minimum	73.699 Pa	71.699 Pa
2	Y-joint	Maximum	101.45 Pa	118.45 Pa
		Minimum	53.778 Pa	53.770 Pa
3	T-joint	Maximum	138.72 Pa	148.72 Pa
		Minimum	51.917 Pa	51.917 Pa

#### 3.2.2.1 Equivalent (von mises) stress of E-glass and S-glass elbow joint:

As shown in Figure 6 above, the maximum value of the von mises equivalent stress of E-glass elbow joint is 99.924  $\text{Nm}^{-2}$  and that of S-glass is 98.904  $\text{Nm}^{-2}$ .

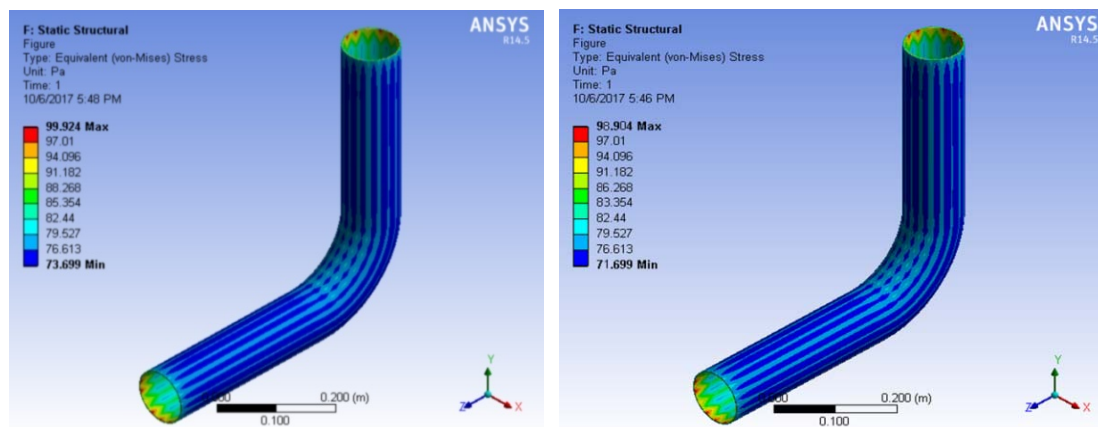


Figure 6 Contours of von mises equivalent stress during 100% crude oil flow with maximum pressure in the elbow joint

#### 3.2.2.2 Equivalent (von mises) stress of E-glass and S-glass Y-joint

As shown in Figure 7 above, the maximum value of the von mises equivalent stress of E-glass Y-joint is 118.45  $\text{Nm}^{-2}$  and that of S-glass is 101.45  $\text{Nm}^{-2}$ .

#### 3.2.2.3 Equivalent (von mises) stress of E-glass and S-glass T-joint

As shown in Figure 8 above, the maximum value of the von Mises Equivalent stress of E-glass T-joint is 148.72  $\text{Nm}^{-2}$  and that of S-glass is 138.72  $\text{Nm}^{-2}$ .

The comparison of the maximum equivalent von mises stresses and minimum equivalent von mises Stresses of joints with E-glass and S-glass fibre material are shown below in Figure 9. In the case of maximum pressure, the pressure was gradually tend to surge from the initial stage to the final stage, but when it came to the minimum pressure of the joints, the graph of both the joints gradually dropped from the peak stage. However, in both cases, S-glass joints showed better output results when compared to E-glass joints.

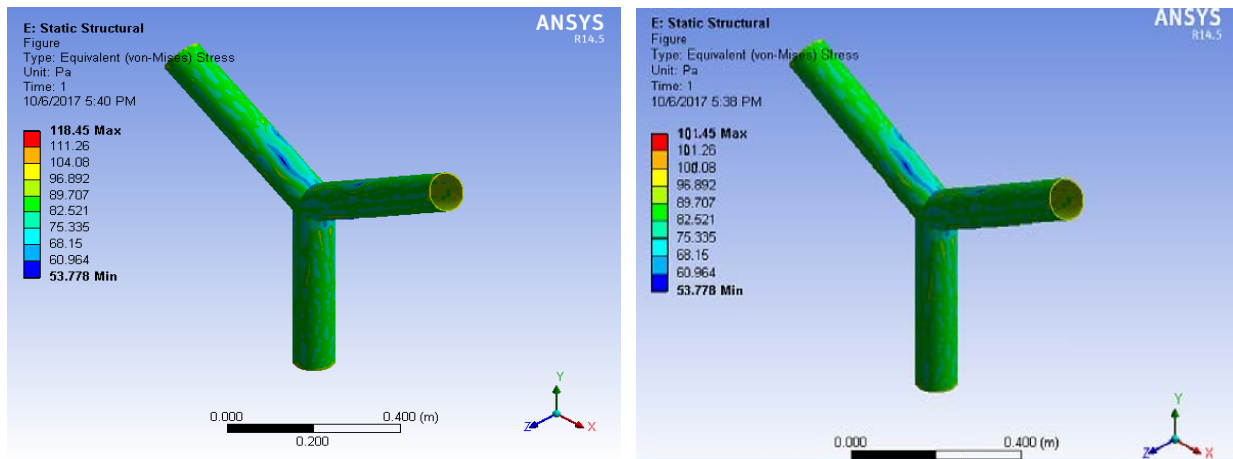


Figure 7 Contours of von mises equivalent stress during 100% crude oil flow with maximum pressure in the Y- joint

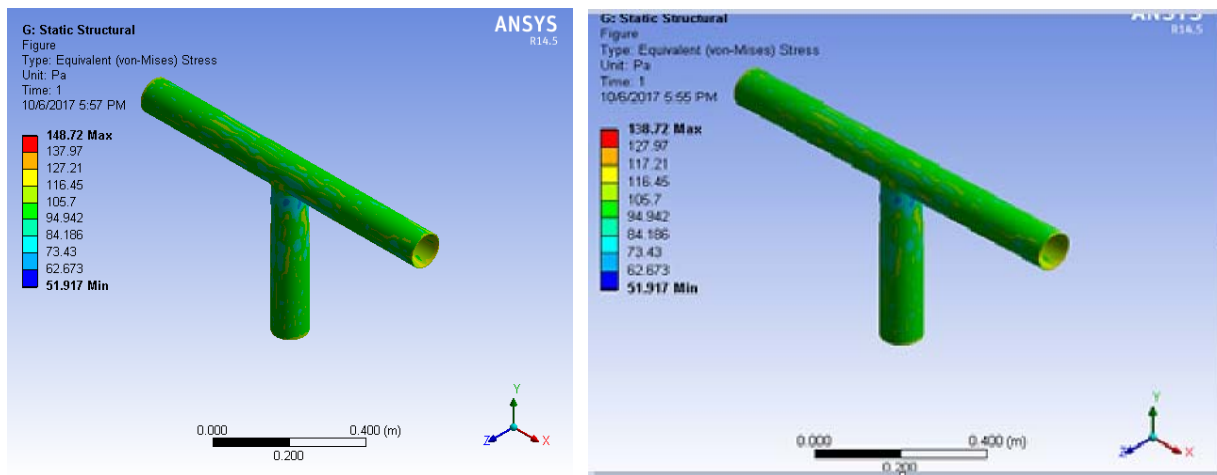


Figure 8 Contours of von mises equivalent stress during 100% crude oil flow with maximum pressure in the T joint

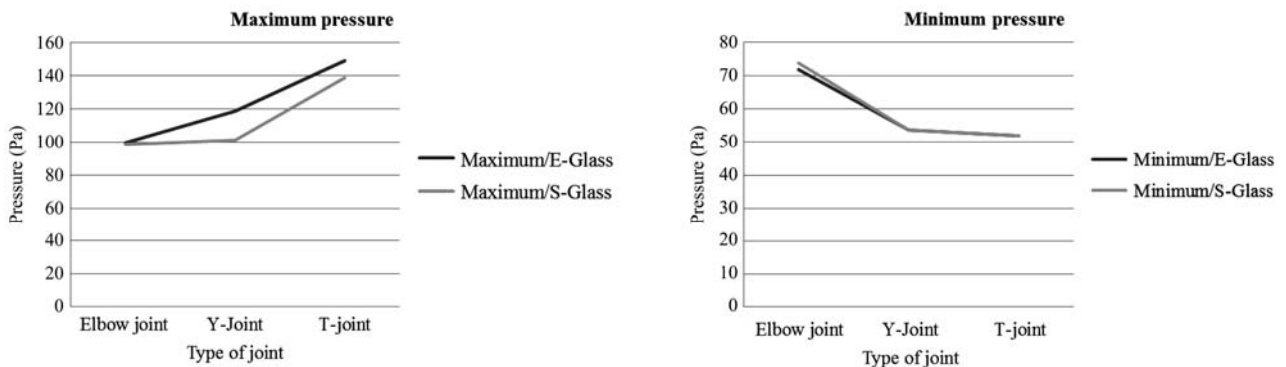


Figure 9 Maximum equivalent (von mises) and minimum equivalent (von mises) stress of various joints with E-glass and S-glass fibre material

When comparing the results obtained from the Ansys 15.0 Structural Analysis and theoretical calculation, the percentage of accuracy are within the permissible limits of the yield strength of the pipe joints, so the design is safe for all the pipe joints.

Since the paper only concentrates on analysis part only material property of E-Glass and S-glass were considered and compared but when it comes to the fabrication part, with E-glass cloth, epoxy resin is coated by hand layup process but in the case of S-glass fabric, a

finishing of N-Matrix type resin N-diglycidyl tribromoaniline (DGTBA) assorted with metaphenylene diamine (MPDA) is proposed for fabrication, since it has good fatigue life as per the examinations carried out by Romans et al. (1972).

#### 4 Results and discussion

There have been several studies on the failure occurrence in pipe joints and their main causes other than pressure variation, material selection but as per the study

done due to the turbulence flow in the pipeline the fluid velocity level in the pipe joints have quite large shear in the flow and structural analysis performed S-glass fiber reinforced pipe joints have exhibited better compressive and flexural behaviour than E-glass fiber reinforced pipe joints. The results of the structural stress levels indicated that joints made with S-glass material would withstand more loads than joints made of E-glass material and also the difference between simulation and theoretical results could logically be even 100% and it was supported by the results obtained and also the results obtained were less than maximum yield strength where the damage happened.

Finally by performing stress examination, it created a good method to estimate the consequences of failure before going into the research laboratory works and also implementing S-glass material in the perfined joints rather than E-glass material enhances the durability of composite pipe in the long time run. They are also several other causes for the failures in glass/epoxy fiber reinforced pipelines which may be due to ecological and physical constraints, but as per the study only flow analysis was performed.

### Conflicts of interest

The authors state that there are no conflicts of interest concerning the publication of this paper.

### References

- Abdul Majid, M. S., A. G. Gibson, M. Hekman, M. Afendi, and N. A. M. Amin. 2014. Strain response and damage modelling of glass/epoxy pipes under various stress ratios. *Plastics, Rubber and Composites*, 43(9): 290–299.
- Akkus, N., and M. Kawahara. 2000. Bending behaviors of thin composite pipes with reinforcing nodes. *Materials Science Research International*, 6(2): 131–135.
- Alderson, K. L., and K. E. Evans. 1992. Failure mechanisms during the transverse loading of filament-wound pipes under static and low velocity impact conditions. *Composites*, 23(3): 167–173.
- Anderson, J. D. 2009. Governing equations of fluid dynamics. In *Computational Fluid Dynamics*, 3rd ed., ed. J. F. Wendt, ch. 2, 15–51. Berlin, Heidelberg: Springer.
- ANSI/AWWA C950-01. 2001. Standard for fiberglass pressure pipe. Denver: American Water Works Association.
- AWWA Manual M45. 2005. Fiberglass pipe design. 2nd ed. Denver: American Water Works Association.
- Bobba, S., Z. Leman, E. S. Zainuddin, and S. M. Sapuan. 2018. Fluid flow analysis of E-glass fiber reinforced pipe joints in oil and gas industry. *AIP Conference Proceedings*, 1952(1): 020018.
- Gay, D., S. V. Hoa, and S. W. Tsai. 2002. *Composite Materials: Design and Applications*. 2nd ed. New York: CRC Press.
- Hilsenkopf, P., B. Boneh, and P. Sollogoub. 1998. Experimental study of behaviour and functional capability of free steel elbows and austenite stainless steel thin walled elbows. *International Journal of Pressure Vessels and Piping*, 33(2): 111–128.
- Hollaway, L. C. 2010. A review of the present and future utilization of FRP composites in the civil infra-structure with reference to their important in-service properties. *Construction and Building Materials*, 24(12): 2419–2445.
- Kim, Y. J., and C. S. Oh. 2007. Effect of attached straight pipes on finite element limit analysis for pipe bends. *International Journal of Pressure Vessels and Piping*, 84(3): 177–184.
- Kleiner, Y., and B. Rajani. 2001. Comprehensive review of structural deterioration of water mains: statistical models. *Urban Water*, 3(3): 131–150.
- Mazumde, Q. H. 2012. CFD analysis of the effect of elbow radius on pressure drop in multiphase flow. *Modelling and Simulation in Engineering*, 2012(37): Article ID 125405.
- Moujaes, S. F., and S. Aekula. 2009. CFD predictions and experimental comparisons of pressure drop effects of turning vanes in 90° duct elbows. *Journal of Energy Engineering*, 135(4): 119–126.
- Nishiwaki, T., A. Yokoyama, Z. I. Maekawa, H. Hamada, and S. Mori. 1995. A quasi-three-dimensional lateral compressive analysis method for a composite cylinder. *Composite Structures*, 32(1-4): 293–298.
- Onoda, J. 1985. Optimal laminate configurations of cylindrical shells for axial buckling. *AIAA Journal*, 23(7): 1093–1098.
- Romans, J. B., A. G. Sands, and J. E. Cowling. 1972. Fatigue behavior of glass filament-wound epoxy composites in water. *Industrial and Engineering Chemistry Product Research and Development*, 11(3): 261–268.
- Shalaby, M. A., and M. Y. A. Younan. 2008. Limit loads for pipe elbows subjected to in-plane opening moments and internal pressure. *Journal of Pressure Vessel Technology*, 121(1): 17–23.
- Smerdov, A. A. 2000. A computational study in optimum formulation of optimization problems on laminated cylindrical shells for buckling: I. Shells under axial compression. *Composites Science and Technology*, 60(11): 2057–2066.
- Xia, M., H. Takayanagi, and K. Kemmochi. 2001. Analysis of transverse loading for laminated cylindrical pipes. *Composite Structures*, 53(3): 279–285.